Diffractive Υ production at the Tevatron and LHC

JHEP06(2009)034

(http://iopscience.iop.org/1126-6708/2009/06/034)

JHEP

Published by IOP Publishing for SISSA

Received: *May 5, 2009*
Accepted: *May 17, 2009*
Published: *June 9, 2009*

Diffractive Υ production at the Tevatron and LHC

B.E. Cox,[a] **J.R. Forshaw**[a] **and R.Sandapen**[b]

[a] *School of Physics & Astronomy, University of Manchester, Oxford Road, Manchester M13 9PL, U.K.*

[b] *Département de Physique et d'Astronomie, Université de Moncton, Moncton, N-B. E1A 3E9, Canada*

E-mail: brian.cox@cern.ch, jeff.forshaw@manchester.ac.uk, ruben.sandapen@umoncton.ca

Abstract: We compute the rate for diffractive Υ meson production at the Tevatron and the LHC. The Υ is produced diffractively via the subprocess $\gamma + p \to \Upsilon + p$ where the initial photon is radiated off an incoming proton (or antiproton). We consider the possibility to use low angle proton detectors to make a measurement of the γp cross-section and conclude that a measurement of the cross-section at a centre of mass energy in excess of 1 TeV is possible at the LHC. This is in the region where saturation effects are likely to reveal themselves.

Keywords: QCD Phenomenology

ArXiv ePrint: 0905.0102

doi:10.1088/1126-6708/2009/06/034

JHEP06(2009)034

Contents

1 Introduction

In this paper we calculate the rate for the reaction $p+p \to p+\Upsilon(nS)+p$ where $n = 1, 2, 3$. The Υ is produced diffractively after one of the incoming protons radiates a photon, as illustrated in figure 1, i.e. via the sub-process $\gamma + p \to \Upsilon + p$.

The reaction is interesting primarily because the LHC will probe values of the γp centre-of-mass energy well beyond those that were reached at HERA. As a result, there is an opportunity to examine QCD in the region where non-linear (saturation) effects are expected to be important. In addition, the odderon is expected to contribute at some level and an accurate measurement would help to constrain the theory. We shall not consider the odderon in this paper.

Ordinarily this is a measurement that could only be performed at low LHC luminosities ($\sim 10^{31}$ cm^{-2}s^{-1}) in order to avoid problems with pileup. However, there is interest in supplementing the LHC general purpose detectors with low angle proton detectors at 420 m from the interaction points; the primary goal being the study of 'central exclusive' production of new physics, and in particular the reaction $p+p \to p+H+p$ [1]. The Υ states are too light to be produced in conjunction with two measured protons but measurement of one proton is feasible and that may be sufficient to control pileup induced backgrounds at instantaneous luminosities in excess of (10^{33} cm^{-2}s^{-1}). Work is currently in progress to measure exclusive Υ production at the Tevatron [2] and the CDF collaboration has identified centrally produced charm meson states [3] and centrally produced dileptons [4].

There already exist a number of papers predicting the rate for this process [5–10]. We add to what has been done by providing predictions using the dipole model cross-section of [11] that successfully describes a wide range of the HERA data [12]. We also make an estimate of the effect of detector acceptances and the impact of measuring one of the protons.

In the following section we explain how to calculate the rate for this process. The flux of photons off an incoming proton is well known, as is the dipole cross-section that determines how the photon produces the Υ after first fluctuating into a $\bar{q}q$ pair. The latter is well determined,[1] primarily as a result of high quality data on the deep inelastic structure

[1] At least for light quark scattering.

JHEP06(2009)034

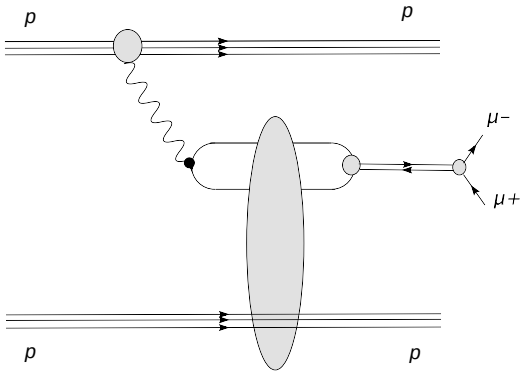

Figure 1. Diffractive photoproduction of the Υ meson in pp collisions. At the Tevatron one p stands for an antiproton and the other for a proton while at the LHC, both stand for protons. The Υ decays into a $\mu^+\mu^-$ pair which is detected. At the LHC, there is opportunity to also detect one of the protons.

function F_2 measured at HERA [13, 14]. In section 3, we compute the photoproduction cross-section and compare our predictions with the available HERA data. In section 4, we present our predictions for the rapidity distributions of the Υ and the expected rates at the Tevatron and the LHC, including the effects of proton tagging.

2 The *pp* cross-section

Entirely in analogy to photoproduction at HERA, where almost on-shell photons are radiated off incoming electrons according to the Weiszäcker-Williams distribution, protons at the LHC can radiate almost real photons that can then scatter off protons heading in the opposite direction. A significant fraction of these γp reactions will be diffractive and leave the incoming proton intact. Amongst these will be the process $\gamma + p \to V + p$ where V is a vector meson and that is where our interest lies.

If the Υ is produced at rapidity Y then its energy $E_\Upsilon \approx M_\Upsilon \cosh Y$ (we neglect the transverse momentum of the meson). Defining

$$\xi = \frac{M_\Upsilon}{\sqrt{s}} \mathrm{e}^Y \tag{2.1}$$

where $\sqrt{s}$ is the center-of-mass energy of the pp system, the cross-section of interest is

$$\frac{\mathrm{d}^2\sigma(pp \to p\Upsilon p)}{\mathrm{d}Y \mathrm{d}Q^2} = \xi f_{\gamma/p}(\xi, Q^2)\, \sigma_{\gamma p}(\xi s) + (\ Y \to -Y\ )\,, \tag{2.2}$$

where $f_{\gamma/p}(\xi, Q^2)$ is the photon flux given by [15]:

$$f_{\gamma/p}(\xi, Q^2) = \frac{\alpha_{\mathrm{em}}}{2\pi} \frac{1 + (1-\xi)^2}{\xi} \frac{1}{Q^2} \frac{1}{\left(1 + Q^2/\mu^2\right)^4}\,, \tag{2.3}$$

and $\mu^2 = 0.71\,\mathrm{GeV}^2$ fixes the electromagnetic form factor of the proton. ξ is the fractional energy loss of the proton. The cross-section for $\gamma + p \to \Upsilon + p$ is denoted by $\sigma_{\gamma p}(W^2)$ where

JHEP06(2009)034

W is the γp centre of mass energy, i.e $W^2 = M_\Upsilon\sqrt{s}\exp(\pm Y)$. W is not uniquely defined by the Υ's rapidity since any one of the two incoming protons can radiate the photon.[2] The two terms on the right-hand-side of eq. (2.2) allow for both possibilities.[3]

The minimum virtuality of the photon is

$$Q^2_{\min} \approx \xi^2 m_p^2\,, \tag{2.4}$$

where m_p is the proton mass. Integrating eq. (2.3) over Q^2 yields the integrated flux [15]:

$$f_{\gamma/p}(\xi) = \frac{\alpha_{\rm em}}{2\pi}\frac{1+(1-\xi)^2}{\xi}\left(\ln A(\xi) - \frac{11}{6} + \frac{3}{A(\xi)} - \frac{3}{2A(\xi)^2} + \frac{1}{3A(\xi)^3}\right) \tag{2.5}$$

with

$$A(\xi) = 1 + \mu^2/Q^2_{\min} \tag{2.6}$$

and thus the rapidity distribution of the Υ is given by

$$\frac{{\rm d}\sigma(pp\to p\Upsilon p)}{{\rm d}Y} = \xi f_{\gamma/p}(\xi)\;\sigma_{\gamma p}(\xi s) + (\;Y\to -Y\;)\;. \tag{2.7}$$

So much for the photon flux, we are now ready to tackle the cross-section for $\gamma + p \to \Upsilon + p$. If the invariant mass $W^2 \gg M^2_\Upsilon$ then we are in the diffractive regime and consequently the imaginary part of the forward ($t = 0$) amplitude can be approximated by:[4]

$$\Im{\rm m}\;\mathcal{A}_{\gamma p}(W^2) = \frac{1}{2}\sum_{\lambda,h,\bar h}\int {\rm d}^2r\;{\rm d}z\;\psi^{\Upsilon *}_{\lambda,h\bar h}(z,r)\psi^{\gamma}_{\lambda,h\bar h}(z,r)\sigma(x,r)\,, \tag{2.8}$$

where $\psi^{\gamma}_{\lambda,h\bar h}(z,r)$ and $\psi^{\Upsilon}_{\lambda,h\bar h}(z,r)$ are the light-cone wavefunctions of the photon and the Υ (of helicity λ). They represent the amplitude for the vector meson to fluctuate into a $b\bar b$ pair of transverse size r and with the quark carrying energy fraction z and helicity $h = \pm\frac{1}{2}$. We take $x = M^2_\Upsilon/W^2$.

The cross-section $\sigma(x,r)$ is called the dipole cross-section and it represents the cross-section for the $b\bar b$ pair to scatter off a proton. The formalism we are describing has been very successful in explaining a very wide range of HERA data, including the extremely precise data on the F_2 structure function at low x [12]. The dipole cross-section has been extracted, for light-quark dipoles, from HERA data and we use a parameterization introduced in [11]; we shall turn to this shortly. First we address the calculation of the light-cone wavefunctions.

The photon wavefunction is well known and, since the longitudinal wavefunction of a real photon vanishes, we shall only need the transverse ($\lambda = \pm 1$) photon wavefunction given by

$$\begin{aligned}\psi^{\gamma}_{\lambda,h\bar h}(z,r) =& \sqrt{\frac{N_{\rm C}}{4\pi}}\sqrt{2}\frac{ee_f}{2\pi}\{\delta_{h,\bar h}\delta_{\lambda,2h}m_bK_0(m_br)\\ &- i(2h)\delta_{h,-\bar h}{\rm e}^{i\lambda\phi}\left[(1-z)\delta_{\lambda,-2h} + z\delta_{\lambda,2h}\right]m_bK_1(m_br)\}\,,\end{aligned} \tag{2.9}$$

[2] Except at $Y = 0$.

[3] By adding cross-sections, we are neglecting the interference between the two amplitudes.

[4] We assume that the Υ retains the helicity of the photon.

JHEP06(2009)034

where $e^2 = 4\pi\alpha_{\rm em}$ and $e_f = -1/3$ is the electric charge of the b quark.

The vector meson wavefunction is less well known. Various models are discussed in [16] and here we shall use the boosted gaussian wavefunction, which works well for the light mesons, ρ and ϕ [16], and also for the heavier J/Ψ meson [12]. In this model, the meson light-cone wavefunction is given by

$$\begin{aligned}\psi^{\Upsilon}_{\lambda,h\bar{h}}(z,r) =& \sqrt{\frac{N_{\rm C}}{4\pi}}\frac{\sqrt{2}}{z(1-z)}\{\delta_{h,\bar{h}}\delta_{\lambda,2h}m_b \\ &+ i(2h)\delta_{h,-\bar{h}}e^{i\lambda\phi}\left[(1-z)\delta_{\lambda,-2h} + z\delta_{\lambda,2h}\right]\partial_r\}\phi_{nS}(z,r)\,, \end{aligned} \tag{2.10}$$

where $\phi_{nS}(z,r)$ is obtained by boosting a Schrödinger gaussian wavefunction using the Brodsky-Huang-Lepage prescription [17]:

$$\phi_{\rm sch}(\mathbf{p}^2) \to \phi_{nS}\left(\frac{\mathbf{k}^2+m_b^2}{4z(1-z)} - m_b^2\right) \tag{2.11}$$

and $\mathbf{p}$ is the relative three-momentum between the quark and antiquark in the meson's rest frame while $\mathbf{k}$ is their relative transverse momentum in the boosted frame. The subscript nS reminds us we are to treat the different Υ states seperately. After a two-dimensional Fourier transformation of the resulting light-cone wavefunction to transverse $\mathbf{r}$-space, we obtain

$$\phi_{nS}(r,z) = \left[\sum_{k=0}^{n-1}\alpha_{nS,k}\; R_{nS}^2\; \hat{D}^{2k}(r,z)\right] G_{nS}(r,z) \tag{2.12}$$

with $\alpha_{nS,0} = 1$. The operator

$$\hat{D}(r,z) = \frac{m_f^2 - \nabla_r^2}{4z(1-z)} - m_f^2 \tag{2.13}$$

with $\nabla_r^2 = \frac{1}{r}\partial_r + \partial_r^2$, acts on the Gaussian function

$$G_{nS}(r,z) = \mathcal{N}_{nS}\; z(1-z)\exp\left(-\frac{m_b^2R_{nS}^2}{8z(1-z)}\right)\exp\left(-\frac{2z(1-z)r^2}{R_{nS}^2}\right)\exp\left(\frac{m_b^2R_{nS}^2}{2}\right). \tag{2.14}$$

Explicitly we obtain[5]

$$\phi_{1S}(r,z) = G_{1S}(r,z)\;, \tag{2.15}$$

$$\phi_{2S}(r,z) = G_{2S}(r,z)[1 + \alpha_{2S,1}\; g_{2S}(r,z)] \tag{2.16}$$

and

$$\phi_{3S}(r,z) = G_{3S}(r,z)\left\{1 + \alpha_{3S,1}\; g_{3S}(r,z) + \alpha_{3S,2}\left[g_{3S}^2(r,z) + 4\left(1 - \frac{4z(1-z)r^2}{R_{3S}^2}\right)\right]\right\}, \tag{2.17}$$

where

$$g_{nS}(r,z) = 2 - m_f^2R_{nS}^2 + \frac{m_f^2R_{nS}^2}{4z(1-z)} - \frac{4z(1-z)r^2}{R_{nS}^2}\,. \tag{2.18}$$

JHEP06(2009)034

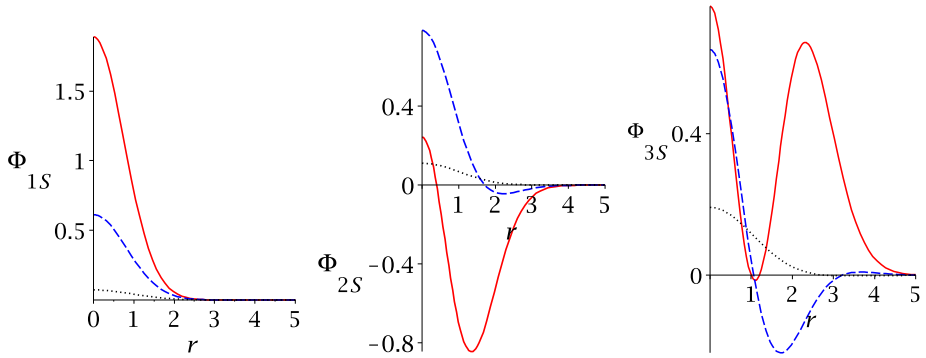

Figure 2. The scalar part of the light-cone wavefunction for $\Upsilon(1S)$ (left), $\Upsilon(2S)$ (center) and $\Upsilon(3S)$ (right) as a function of the transverse size, r (GeV^{-1}), of the $b\bar{b}$ pair with the light-cone momentum fraction carried by the quark, $z = 0.5$ (solid), $z = 0.3$ (dashed) and $z = 0.2$ (dotted).

Boosted Gaussian parameters

n	R^2_{nS}	$\alpha_{nS,1}$	$\alpha_{nS,2}$	$\mathcal{N}_{nS}$	$\Gamma_{e^+e^-}$	$\Gamma^{\rm exp}_{e^+e^-}$
1	0.567	.	.	0.481	1.340	1.340 ± 0.018
2	0.831	-0.555	.	0.624	0.611	0.612 ± 0.011
3	1.028	-1.219	0.217	0.668	0.443	0.443 ± 0.008

Table 1. Parameters and predicted electronic decay widths of the Boosted Gaussian light-cone wavefunctions in appropriate GeV based units. The decay widths are given in keV. Experimental values are taken from [19] and we take $m_b = 4.2$ GeV.

The scalar wavefunctions ϕ_{1S}, ϕ_{2S} and ϕ_{3S} are shown in figure 2 for $z = 0.2, 0.3$ and 0.5.

The parameters $\alpha_{nS,k}$ (for $k > 0$) have been fixed by requiring that the wavefunctions of different states be orthogonal to each other. The values of R_{nS} are fixed so as to reproduce the experimentally measured electronic decay widths [16]. The values of the parameters thus obtained, together with the predicted decay widths, are given in table 1 and the resulting wavefunctions are shown in figure 3.

It remains to specify the parametric form of the dipole cross-section. Here we use the saturation model presented in [11] (which we subsequently refer to as the "FSSat" model). It has the following form:

$$\begin{aligned} \sigma(x,r) &= A_H r^2 x^{-\lambda_H} && \text{for } r < r_0 \text{ and} \\ &= A_S x^{-\lambda_S} && \text{for } r > r_1. \end{aligned} \tag{2.19}$$

In the intermediate region $r_0 \le r \le r_1$, the dipole cross-section is determined by interpolating linearly between the two forms of eq. (2.19). r_0 is fixed to be the value at which the hard component is some specified fraction of the soft component, i.e.

$$\sigma(x, r_0)/\sigma(x, r_1) = f\,, \tag{2.20}$$

[5] We note that if the double partial derivative ∂_r^2 is used in eq. (2.13) instead of the Laplacian operator, ∇_r^2, the $2S$ wavefunction reduces to that presented in [18].

JHEP06(2009)034

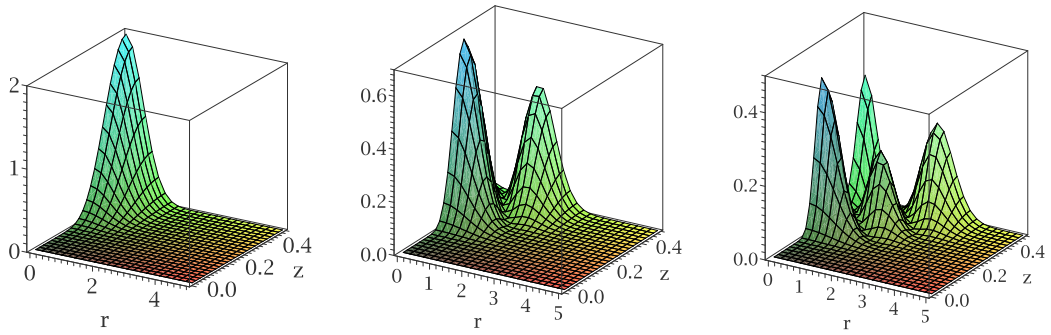

Figure 3. The light-cone wavefunction squared, $|\Psi^{\Upsilon}|^2$, for the transversely polarised $\Upsilon(1S)$ (left), $\Upsilon(2S)$ (center) and $\Upsilon(3S)$ (right) as a function of the transverse size, r (GeV^{-1}), of the $b\bar{b}$ pair and the light-cone momentum fraction, z, carried by the quark.

where f is treated as a parameter that is determined, along with the other parameters $A_S, A_H, \lambda_S, \lambda_H$ and r_1, by a fit to the total structure function F_2 data from HERA [11].

We now have almost all of the ingredients we need in order to compute the amplitude (2.8) for Υ production. The forward differential cross-section is given by

$$\left.\frac{\mathrm{d}\sigma_{\gamma p}}{\mathrm{d}t}\right|_{t=0} = \frac{1}{16\pi}|\mathcal{A}_{\gamma p}|^2 \tag{2.21}$$

and the total cross-section is obtained by assuming an exponential fall-off with increasing $|t|$, i.e

$$\sigma_{\gamma p} = \frac{1}{B_\Upsilon}\left.\frac{\mathrm{d}\sigma_{\gamma p}}{\mathrm{d}t}\right|_{t=0}, \tag{2.22}$$

where the diffractive slope, B_Υ, is taken to be [16]

$$B_\Upsilon = N\left(\frac{14.0}{(M_\Upsilon/\mathrm{GeV})^{0.4}} + 1\right) = 3.68\ \mathrm{GeV}^{-2} \tag{2.23}$$

with $N = 0.55\,\mathrm{GeV}^{-2}$. Before presenting our predictions for hadron-hadron collisions, we shall first compute the photon-proton cross-section $\sigma_{\gamma p}$ and compare it to existing HERA data.

3 The γp cross-section

To compare to the data, we compute

$$\sigma^*_{\gamma p} = \sum_{n=1}^{3} \sigma_{\gamma p \to \Upsilon(nS)p} \times B_n\,, \tag{3.1}$$

where B_n is the branching ratio of the $\Upsilon(nS)$ to muons. In figure 4, we compare our predictions to the HERA data [20–22].

As can be seen, the theory curve (dotted) lies significantly below the HERA data. However, we have ignored two important corrections. The first is the contribution from

JHEP06(2009)034

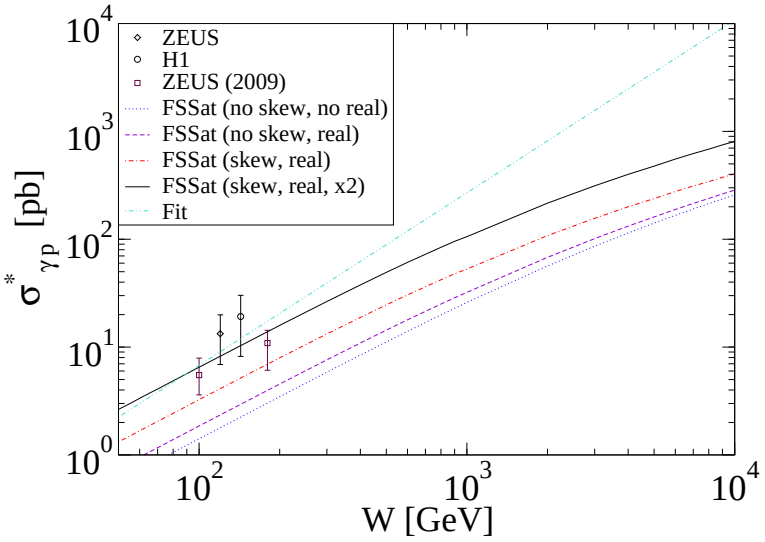

Figure 4. Predictions for the γp cross-section. Dotted curve — no skewedness correction and without the real part; dashed curve — including the real part; dot-dashed curve — including the real part and a skewedness correction. The solid curve is the dot-dashed curve normalised to the HERA data and the double-dot-dashed curve is the parameterization to the HERA data described in the text [6].

the real part of the amplitude and including it increases the cross-section for each state by a factor of $(1+\beta^2)$ where β is the ratio of the real to imaginary part of the γp amplitude, given by

$$\beta = \tan\left(\frac{\pi}{2}\lambda\right) \tag{3.2}$$

with

$$\lambda = \frac{\partial \ln |\Im\mathrm{m}\, \mathcal{A}|}{\partial \ln (1/x)} \tag{3.3}$$

where $\Im\mathrm{m}\, \mathcal{A}$ is given by eq. (2.8).

Figure 5 shows the ratio of the real to imaginary parts of the amplitude for each state. We note that the calculation of this ratio is model-dependent especially for the higher states. The dashed curve in figure 4 shows the effect of including the correction due to the real part.

The second correction arises because the amplitude is not diagonal — the mass of the Υ is large and timelike compared to the small, spacelike, photon virtuality. In contrast, our dipole scattering cross-section was extracted from data at zero momentum transfer. We estimate the corrections from this source by multiplying the amplitude by a factor of [23]

$$R_g(\lambda) = \frac{2^{2\lambda+3}}{\sqrt{\pi}} \frac{\Gamma(\lambda+5/2)}{\Gamma(\lambda+4)} \ . \tag{3.4}$$

Our prediction, with this correction included, is shown in figure 4 as the dot-dashed curve.

A few comments are in order regarding our estimation of the above two corrections. Both of them depend on λ, which we estimate using eq. (3.3). We have checked that

JHEP06(2009)034

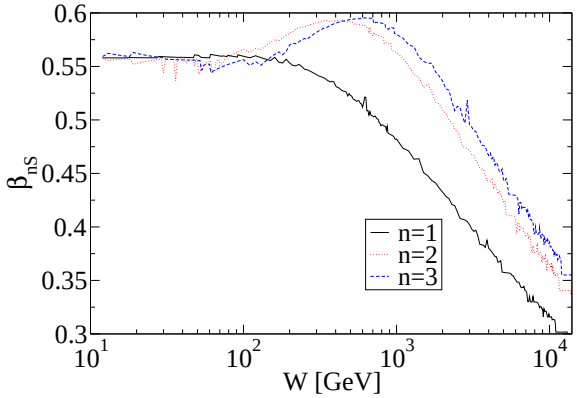

Figure 5. The ratio of the real to imaginary part of the amplitude for the different states.

our results do not vary very much upon choosing a fixed value of $\lambda = 0.3$. Since the Υ wavefunction extends to larger r for the excited states, relative to that of the $1s$ state (see figure 3), one might naively expect that the energy dependence is softer for the former, resulting in a lower effective value of λ. This is actually not the case as one can infer from figure 5. This is because the excited state wavefunctions have nodes, which leads to a partial cancellation between the soft and hard parts of the amplitude which in turn results in an effective harder energy dependence (higher λ) in the amplitudes. The degree of cancellation is rather sensitive to the model used for the dipole cross-section. This has been referred to previously as the node effect [18].

Even with these corrections, the theory curve still lies below the data. This is not a particularly surprising result and it is typical of other dipole model calculations [6, 24]. Quite possibly, one could do better by improving the vector meson wavefunctions and in that case the uncertainty would mainly influence the normalisation of the cross-section. Moreover, the value chosen for the b quark mass also affects the overall normalisation. For these reasons, we follow the authors of [6] and rescale our results (by a factor 2.0 with $m_b = 4.2\,\mathrm{GeV}$) in order to achieve optimum agreement with the data. The result is the solid curve in figure 4. By doing this, we account also for the uncertainties in the real part and skewedness corrections in a purely phenomenological way.

In [6], the parametrisation

$$\sigma = 0.12 \text{ pb } \times \left(\frac{W}{\mathrm{GeV}}\right)^{1.6} \tag{3.5}$$

was found to fit the HERA data for $\Upsilon(1S)$. Both H1 and ZEUS measure $\sigma^*_{\gamma p}$ and then extract the $1S$ cross-section by assuming that the ratios of cross-section times branching ratio are the same as those measured by the CDF collaboration [25], i.e. $(\sigma_{2S} \cdot B_{2S})/(\sigma_{1S} \cdot B_{1S}) = 0.281 \pm 0.0484$ and $(\sigma_{3S} \cdot B_{3S})/(\sigma_{1S} \cdot B_{1S}) = 0.155 \pm 0.0319$. We use eq. (3.5), together with the CDF ratios, to produce the double-dot-dashed curve in figure 4.[6]

[6]The original fit of [6] did not include the most recent HERA data. Including it brings the fit down so that it is much closer to the FSSat prediction.

JHEP06(2009)034

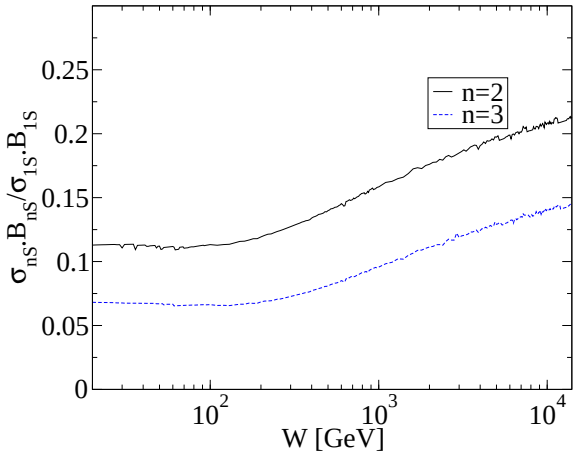

Figure 6. The ratio of cross-sections for the different states.

We can also compute the cross-section ratios between the different Υ states in order to compare to the CDF data. These are shown in figure 6. Our results are below the values obtained by CDF quoted above. For the $2S:1S$ ratio, in the range $50 < W < 200\,\text{GeV}$, our prediction is also below the value calculated in [7] using perturbative QCD and a Gaussian wavefunction. However, theoretical predictions for these ratios are rather uncertain since the $2S:1S$ ratio is very sensitive to the details of the meson wavefunction and also to the value of λ.

Note that the FSSat model predicts an energy dependence that is less steep than the $W^{1.6}$ dependence of the fit. We might take the difference to be indicative of the challenge facing future experiments, i.e. they should be able to distinguish between the two.

4 Results

We are now ready to present our predictions for the hadroproduction cross-section. We assume that the angular distribution of the decay muons in the Υ rest frame is $\propto (1+\cos^2\theta^*)$, which corresponds to a distribution of

$$\frac{\mathrm{d}^2N}{\mathrm{d}(\cos\theta)\mathrm{d}\phi} = \frac{3}{16\pi}\frac{1-\beta^2}{(1-\beta\cos\theta)^2}\left[1+\left(\frac{\cos\theta-\beta}{(1-\beta\cos\theta)}\right)^2\right] \tag{4.1}$$

in the lab: $\beta = \tanh Y$ is the speed of the Υ and θ is the polar angle relative to the direction in which the Υ travels when $\beta > 0$.[7] Thus

$$\frac{\mathrm{d}^2\sigma(pp\to p\{\mu^+\mu^-\}p)}{\mathrm{d}(\cos\theta)\mathrm{d}Y} = \frac{\mathrm{d}N}{\mathrm{d}(\cos\theta)}\xi\sigma_{\gamma p}(\xi s)\; f_{\gamma/p}(\xi) \;+(Y\to -Y)\;. \tag{4.2}$$

We integrate over θ such that both the μ^- and μ^+ are emitted at an angle greater than $\theta_{\min}$ relative to the beam. To do that we need α, the emission angle of the μ^+:

$$\cos\alpha = \frac{(1+\beta^2)\cos\theta - 2\beta}{1+\beta^2-2\beta\cos\theta}\;. \tag{4.3}$$

[7]Recall that we neglect the transverse momentum of the meson, which means it travels along the beam axis.

JHEP06(2009)034

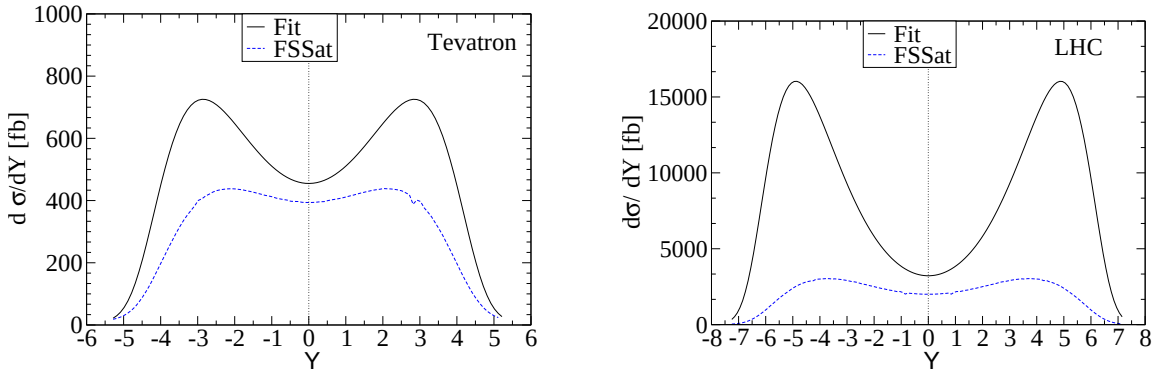

Figure 7. The Υ rapidity distribution without any cuts on the final state particles at the Tevatron (left) and LHC (right) using the FSSat dipole model and the parameterization the photoproduction data described in the text.

The transverse momentum of the muon (or anti-muon) is given by

$$P_t = \frac{M_\Upsilon^2 \sin\theta}{2E_\Upsilon(1-\beta\cos\theta)} \tag{4.4}$$

and we also cut on a minimum value of $P_t^{\min}$ for both leptons.

For the Tevatron, we approximate the angular acceptance of the CDF muon detector using $\theta_{\min} = 33.5°$, whilst for the DØ detector we take $\theta_{\min} = 15.4°$. At the LHC we assume, $\theta_{\min} = 7.7°$ (see also [26]). In all cases we show results for $P_t^{\min} = 3\,\text{GeV}$ and $P_t^{\min} = 4\,\text{GeV}$. At the LHC, we may also have the possibility to detect one of the protons in the region 420 m from the interaction point (there will not be any acceptance to detect both). According to the studies presented in [1], forward detectors in the 420 m region have acceptance for protons with fractional energy loss $0.002 < \xi < 0.018$ on the right-hand side and $0.0015 < \xi < 0.014$ on the left-hand side.

Figure 7 shows the Υ rapidity distributions at the LHC and the Tevatron respectively before any cuts have been applied. There is a striking difference (especially at the LHC) between the shapes of the distributions obtained using the FSSat dipole model and the parameterization of the photoproduction cross-section that is based on the HERA data. One could therefore hope that measurements of the rapidity distributions would be able to discriminate between dipole models and thereby contrain the gluon distribution. In figure 8 we indicate the effect of cutting on the muon p_t and rapidity and, in the case of the LHC, the effect of observing one of the protons in the proposed 420 m detectors. Our results show that although the strong sensitivity to the energy dependence on the dipole cross-section is diminished, it is still large enough that one could hope to constrain the theory.

Tagging one of the protons does severely limit the acceptance of a measurement: Centrally produced mesons are cut out because the 420 m detectors select events in which the measured proton loses much more energy than the unmeasured proton. The boost is so large in fact that the upsilon always travels in the direction of the tagged proton. However, detecting a proton does have the potential advantage that the measurement need not only be performed using data collected at low ($\lesssim 10^{32}\ \text{cm}^{-2}\text{s}^{-1}$) luminosities. With one tagged proton, one could hope to control the pileup background after utilising the fact that the

JHEP06(2009)034

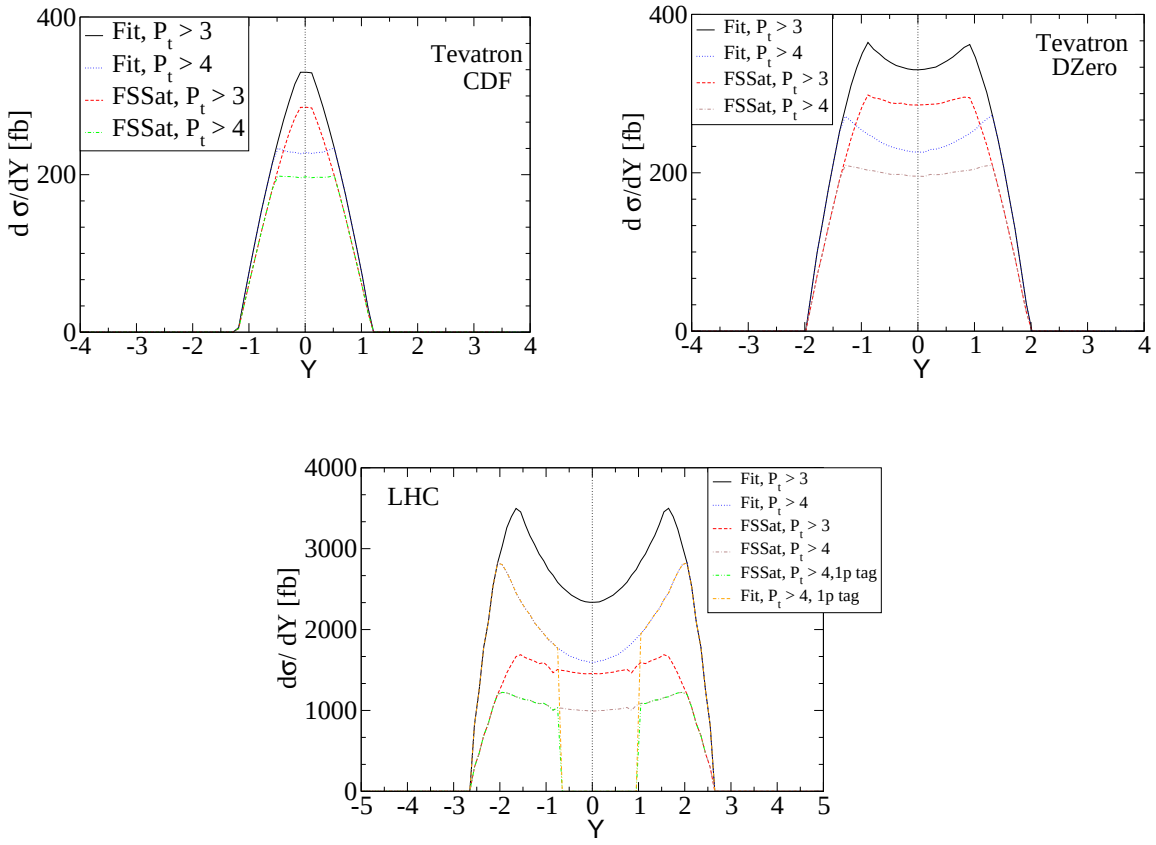

Figure 8. The Υ rapidity distribution after cuts at the Tevatron (top) and LHC (bottom) using the FSSat dipole model and the the parameterization the photoproduction data described in the text.

Cross-sections at the Tevatron

	$\sigma_{\rm FSSat}$(fb)	$\sigma_{\rm Fit}$(fb)
CDF	350	406
DØ	685	838

Table 2. The predicted cross-sections for the Tevatron using the FSSat dipole model (first column) and the power-law fit to the photoproduction data (second column). Cuts on the muon rapidities and transverse momentum have been applied ($P_t > 4\,\text{GeV}$).

two charged muons should point to a single vertex (and no other tracks point to the same vertex) and that they should also combine to produce an Υ rapidity that is in agreement with the value inferred from the extracted (one measured directly and one inferred) proton momentum fractions. Further detailed simulations would be required to establish whether this method will work at 2×10^{33} cm^{-2}s^{-1} and above. In any case, it is worth noting that 10^{32} cm^{-2}s^{-1} corresponds to 1 fb^{-1} per year. That translates to a total of over 5000 signal

JHEP06(2009)034

Cross-sections at the LHC

No. of tagged protons	$\sigma_{\rm FSSat}$(fb)	$\sigma_{\rm Fit}$(fb)
0	5133	10351
1	3035	6802

Table 3. The predicted cross-sections for the LHC using the FSSat dipole model (first column) and the power-law fit to the photoproduction data (second column). Cuts on the muon rapidities and transverse momentum ($P_t > 4\,\text{GeV}$) have been applied (first row). The result of additionally measuring one of the outgoing protons is shown in the second row.

events in an environment where there will be, on average, less than one pp interaction per bunch crossing. This should be sufficient to produce a measurement that will constrain QCD models of saturation.

Finally, it is worth pointing out that should it be possible to make a cut on the measured proton's transverse momentum then it would become possible to make a direct measurement of the photoproduction cross section. This is so since the transverse momentum of protons that radiate photons is typically much smaller than the transverse momentum of protons that do not, i.e. eq. (2.3) is much softer than the $\exp(B_\Upsilon t)$ dependence implied by eq. (2.23). Requiring that the transverse momentum of the tagged proton $p_T < 100\,\text{MeV}$ is at least 60% efficient for selecting events in which the tagged proton radiates a photon.[8] The contamination from events in which the non-tagged proton radiates a photon would be only 4%. If the cut is lifted to 300 MeV, the ratio decreases to 89% : 28%, which still constitutes a very significant enhancement.

After making such a cut, since we now have an enriched sample of events in which the tagged proton radiated the photon, we can eliminate the photon flux and extract the photoproduction cross-section. Figure 9 illustrates the possibilities. The region at larger W (much larger than can be probed at HERA and the Tevatron) is obtained by insisting that the tagged proton p_T be sufficiently small, in which case the tagged proton most likely radiated the photon. The lower W region can be measured by making the complementary cut, i.e. by insisting that the proton have p_T above some value. This is equivalent to assuming that the untagged proton emitted the photon. In this way, the proton detectors facilitate a measurement of the $\gamma p \to \Upsilon p$ cross-section at $W = 1\,\text{TeV}$, which is well in the range where saturation effects are expected to reveal themselves.

So far, we have made no mention of the issue of "gap survival" and as far as the overall rate is concerned it is not expected to provide much suppression, since the collision is typically rather peripheral. However, the gap survival should depend rather strongly on the proton p_T, with gaps being filled in more often at larger values of p_T. Indeed measuring the p_T distribution has been advertised as a means to probe the gap-filling mechanism. This physics would need to be under control before one could reliably extract the photoproduction cross-section by exploiting a p_T cut on the scattered proton [27, 28].

[8] The efficiency depends weakly upon the energy lost by the proton through eq. (2.4).

JHEP06(2009)034

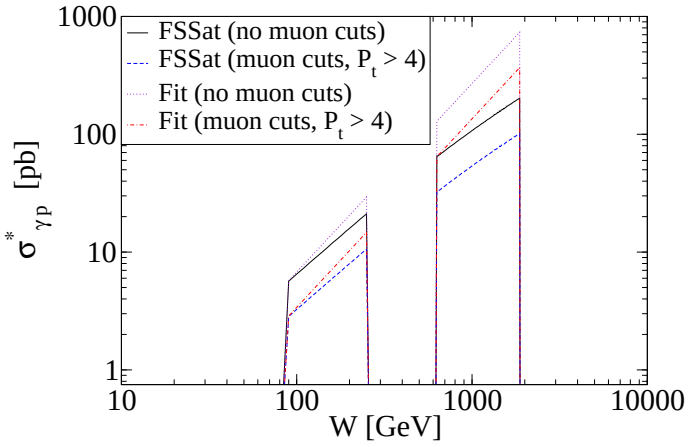

Figure 9. The photoproduction cross-section extracted after cutting on the transverse momentum of the tagged proton.

Acknowledgments

We wish to thank Thorsten Wengler, Andrew Pilkington and Graeme Watt for helpful discussions. We also thank the Royal Society and the STFC for financial support.

References

[1] FP420 R AND D collaboration, M.G. Albrow et al., *The FP420 R&D Project: Higgs and new physics with forward protons at the LHC*, arXiv:0806.0302 [SPIRES].

[2] CDF collaboration, J. Pinfold, *Diffractive and exclusive dilepton and diphoton production at CDF II*, presented at the *XVI international workshop on deep-inelastic scattering and related subjects (DIS08)*, London England U.K., April 7–11 2008.

[3] CDF collaboration, T. Aaltonen et al., *Observation of exclusive charmonium production and gamma+gamma to $\mu^+\mu^-$ in p+pbar collisions at $\sqrt{s} = 1.96$ TeV*, arXiv:0902.1271 [SPIRES].

[4] CDF collaboration, T. Aaltonen et al., *Search for exclusive Z boson production and observation of high mass $p\bar{p} \to \gamma\gamma \to p + \ell\ell + \bar{p}$ events in $p\bar{p}$ collisions at $\sqrt{s} = 1.96$ TeV*, arXiv:0902.2816 [SPIRES].

[5] S.R. Klein and J. Nystrand, *Photoproduction of quarkonium in proton proton and nucleus nucleus collisions*, *Phys. Rev. Lett.* **92** (2004) 142003 [hep-ph/0311164] [SPIRES].

[6] L. Motyka and G. Watt, *Exclusive photoproduction at the Tevatron and LHC within the dipole picture*, *Phys. Rev.* **D 78** (2008) 014023 [arXiv:0805.2113] [SPIRES].

[7] A. Rybarska, W. Schafer and A. Szczurek, *Exclusive photoproduction of upsilon: from HERA to Tevatron*, *Phys. Lett.* **B 668** (2008) 126 [arXiv:0805.0717] [SPIRES].

[8] A. Bzdak, L. Motyka, L. Szymanowski and J.R. Cudell, *Exclusive J/ψ and Υ hadroproduction and the QCD odderon*, *Phys. Rev.* **D 75** (2007) 094023 [hep-ph/0702134] [SPIRES].

[9] D.Y. Ivanov, G. Krasnikov and L. Szymanowski, *Hard exclusive production of a vector meson*, *Nucl. Phys. Proc. Suppl.* **146** (2005) 134 [hep-ph/0412235] [SPIRES].

JHEP06(2009)034

[10] V.P. Goncalves and M.V.T. Machado, *Quarkonium production in coherent hadron-hadron interactions at the LHC*, *Phys. Rev.* **D 77** (2008) 014037 [arXiv:0707.2523] [SPIRES].

[11] J.R. Forshaw and G. Shaw, *Gluon saturation in the colour dipole model?*, *JHEP* **12** (2004) 052 [hep-ph/0411337] [SPIRES].

[12] J.R. Forshaw, R. Sandapen and G. Shaw, *Further success of the colour dipole model*, *JHEP* **11** (2006) 025 [hep-ph/0608161] [SPIRES].

[13] ZEUS collaboration, S. Chekanov et al., *Measurement of the neutral current cross section and F_2 structure function for deep inelastic e^+p scattering at HERA*, *Eur. Phys. J.* **C 21** (2001) 443 [hep-ex/0105090] [SPIRES].

[14] H1 collaboration, C. Adloff et al., *Deep-inelastic inclusive ep scattering at low x and a determination of α_s*, *Eur. Phys. J.* **C 21** (2001) 33 [hep-ex/0012053] [SPIRES].

[15] M. Drees and D. Zeppenfeld, *Production of supersymmetric particles in elastic ep collisions*, *Phys. Rev.* **D 39** (1989) 2536 [SPIRES].

[16] J.R. Forshaw, R. Sandapen and G. Shaw, *Colour dipoles and ρ, ϕ electroproduction*, *Phys. Rev.* **D 69** (2004) 094013 [hep-ph/0312172] [SPIRES].

[17] S.J. Brodsky, T. Huang and G.P. Lepage, *The hadronic wave function in quantum chromodynamic*, SLAC-PUB-2540 (1980), shorter version contributed to *20th int. conf. on high energy physics*, Madison Wisc. U.S.A., July 17–23 1980.

[18] J. Nemchik, N.N. Nikolaev, E. Predazzi and B.G. Zakharov, *Color dipole phenomenology of diffractive electroproduction of light vector mesons at HERA*, *Z. Phys.* **C 75** (1997) 71 [hep-ph/9605231] [SPIRES].

[19] Particle Data Group collaboration, C. Amsler et al., *Review of particle physics*, *Phys. Lett.* **B 667** (2008) 1 [SPIRES].

[20] ZEUS collaboration, J. Breitweg et al., *Measurement of elastic Υ photoproduction at HERA*, *Phys. Lett.* **B 437** (1998) 432 [hep-ex/9807020] [SPIRES].

[21] H1 collaboration, C. Adloff et al., *Elastic photoproduction of J/ψ and Υ mesons at HERA*, *Phys. Lett.* **B 483** (2000) 23 [hep-ex/0003020] [SPIRES].

[22] ZEUS collaboration, S. Chekanov et al., *Exclusive photoproduction of Υ mesons at HERA*, DESY-09-036 March 2009.

[23] A.G. Shuvaev, K.J. Golec-Biernat, A.D. Martin and M.G. Ryskin, *Off-diagonal distributions fixed by diagonal partons at small x and ξ*, *Phys. Rev.* **D 60** (1999) 014015 [hep-ph/9902410] [SPIRES].

[24] ZEUS collaboration, J.T. Malka, *Υ production and DVCS*, presented at the *XVI international workshop on deep-inelastic scattering and related subjects (DIS08)*, London England U.K., April 7–11 2008.

[25] CDF collaboration, F. Abe et al., *Υ production in $p\bar{p}$ collisions at $\sqrt{s} = 1.8$ TeV*, *Phys. Rev. Lett.* **75** (1995) 4358 [SPIRES].

[26] CMS collaboration, *Exclusive dilepton production*, CMS PAS DIF-07-001.

[27] V.A. Khoze, A.D. Martin and M.G. Ryskin, *Photon exchange processes at hadron colliders as a probe of the dynamics of diffraction*, *Eur. Phys. J.* **C 24** (2002) 459 [hep-ph/0201301] [SPIRES].

[28] V.A. Khoze, A.D. Martin and M.G. Ryskin, *Early LHC measurements to check predictions for central exclusive production*, *Eur. Phys. J.* **C 55** (2008) 363 [arXiv:0802.0177] [SPIRES].

JHEP06(2009)034